TEMPERATURE AND ENTROPY PROFILES OF NEARBY COOLING FLOW CLUSTERS OBSERVED WITH XMM-NEWTON AND THE EFFERVESCENT HEATING MODEL

R. Piffaretti[1], J. S. Kaastra[2], Ph. Jetzer[3], and T. Tamura[4]

[1]Institute for Astrophysics, Leopold-Franzens University of Innsbruck, Technikerstraße 25, A-6020 Innsbruck, Austria
[2]SRON National Institute for Space Research, Sorbonnelaan 2, 3584 CA Utrecht, The Netherlands
[3]Institute of Theoretical Physics, University of Zürich, Winterthurerstrasse, 190, CH-8057 Zürich, Switzerland
[4]Institute of Space and Astronautical Science, 3-1-1 Yoshinodai, Sagamihara, Kanagawa 229-8510, Japan

ABSTRACT

We present temperature and entropy profiles of 13 nearby cooling flow clusters observed with *XMM-Newton*. When normalized and scaled by the virial radius the temperature profiles turn out to be remarkably similar and at large radii the temperature profiles show a clear decline. The entropy S of the plasma increases monotonically moving outwards almost proportional to the radius. The dispersion in the entropy profiles is smaller if the empirical relation $S \propto T^{0.65}$ is used instead of the standard self-similar relation $S \propto T$ and no entropy cores are observed. In addition to these results we present recent observational constraints on the "effervescent heating" model derived from *XMM-Newton* observations of 16 cooling flow clusters.

Key words: ESA; X-rays; Cluster of galaxies; cooling flows.

1. INTRODUCTION

Temperature and entropy profiles of the X-ray-emitting intracluster medium (ICM) provide crucial information on the thermodynamic history of the plasma and the comparison between observed profiles and theoretical predictions is an essential test for any model of structure formation of groups and clusters of galaxies. Cooling flow (CF) clusters are of particular interest: gas cooling is of great importance in their cores, since the gas is dense enough to radiate an amount of energy equal to its thermal energy in less than a billion years. *XMM-Newton* observations have greatly improved our understanding of CF clusters. In Sects. 2 and 3 we show results from spatially resolved spectroscopy for a sample of nearby CF clusters observed with *XMM-Newton* and comment on the shape of temperature and entropy radial profiles, respectively. *XMM-Newton* spectra failed to detect the emission lines that dominate the emission from gas below 2 keV (e.g., Peterson et al. (2003)), therefore ruling out the standard CF model. Spatially resolved spectroscopy shows that the temperature in CF clusters drops towards the center to approximatively one third of the cluster mean temperature, indicating that the gas is prevented from cooling below these cutoff temperatures (Kaastra et al. (2004) and Sect. 2). This recent evidence of lack of cool gas shows that the dynamics of the ICM in CF clusters in not solely governed by cooling of the ICM and that some heating mechanisms must be investigated. Recent observations of the interaction between active galactic nuclei (AGN) at the center of CF clusters with the surrounding gas (i.e., Blanton (2004)), has motivated the development of models incorporating AGN feedback. Ruszkowski & Begelman (2002) (RB02, hereafter) have recently proposed such a model, which in addition to AGN heating incorporates heating by thermal conduction. In Sect. 4 we investigate whether RB02's model (or effervescent heating model, hereafter) can provide a satisfactory explanation of the observed structure of CF clusters using *XMM-Newton* observations.

2. TEMPERATURE PROFILES

Various observational studies have found different and conflicting results regarding temperature gradients in the outer regions of galaxy clusters. In Piffaretti et al. (2005) we have investigated temperature profiles of 17 cooling flow clusters using the results from the spatially resolved spectra taken with the EPIC cameras of *XMM-Newton* (Kaastra et al. (2004)). In Fig. 1, we present the deprojected radial profiles of 13 clusters plotted against the radius in units of $r_{\rm vir}$ ($\approx r_{101}$ for ΛCDM cosmology at $z = 0$), where the temperature has been normalized by the mean emission-weighted temperature $< T_{\rm X} >$. The virial radius has been computed from the mass profile determined through the assumption of hydrostatic equilibrium and spherical symmetry. For 4 objects (Virgo, MKW 9, Hydra A and A 399) this estimate is not possible and therefore their scaled profiles are not presented.

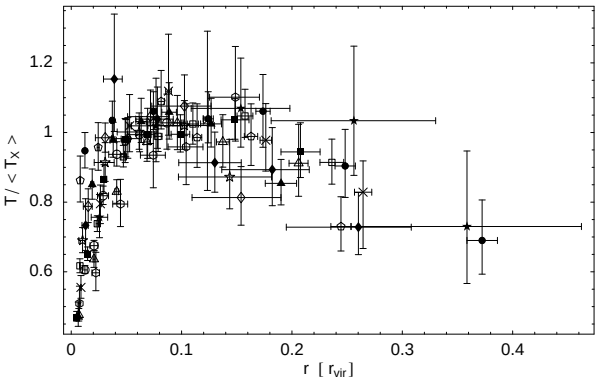

Figure 1. Scaled temperature profiles (deprojected) in a ΛCDM70 cosmology ($\Omega_{\rm m} = 0.3$, $\Omega_\Lambda = 0.7$, with $H_0 = 70\ km\,s^{-1}\,Mpc^{-1}$). The radius is scaled with the virial radius $r_{\rm vir}$, while the temperature is normalized by the mean emission-weighted temperature $< T_{\rm X} >$. Clusters are related to symbols as follows: NGC 533 (crosses), A 262 (filled squares), A 1837 (filled diamonds), Sérsic 159−3 (filled circles), 2A 0335+096 (open triangles), MKW 3s (open pentagons), A 2052 (filled triangles), A 4059 (open diamonds), A 496 (open hexagon), A 3112 (open stars), A 1795 (open squares), Perseus (open circles) and A 1835 (filled stars).

From a visual inspection of Fig. 1 it is evident that a temperature gradient is present at large radii and that when normalized and scaled by the virial radius, temperature profiles are remarkably similar. The individual profiles clearly show a break radius $r_{\rm br}$, a decrease of temperature from $r_{\rm br}$ inwards typical of CF clusters, and the decline at radii larger than $r_{\rm br}$. We have measured the break radius in units of the virial radius for each individual object and we find a mean value $r_{\rm br} \sim 0.09\, r_{\rm vir}$ with a standard deviation of 0.01. We have compared our scaled profiles with the results of Markevitch et al. (1998), De Grandi & Molendi (2002) and Vikhlinin et al. (2005), since these are studies which used fairly large samples and a scaling procedure similar to ours, and found good agreement. The size of our sample, along with the good temperature determination within the cooling radius, allows us to study the shape of the profiles in this region. We have modeled the central temperature drop using:

$$T(r) = T_c + (T_h - T_c)\frac{(r/r_{\rm c})^2}{1 + (r/r_{\rm c})^2}, \qquad (1)$$

with $T_{\rm c}$ set equal to the temperature of the innermost bin. We have fitted each individual and determined the best fit parameters $T_{\rm h}$ and $r_{\rm c}$. A correlation between the fitting parameters of the form $r_c \propto T_h^{1.84\pm0.14}$, with r_c in kpc and T_h in keV, is found. Assuming that r_Δ scales with $T_h^{1/2}$ (i.e., the size-temperature relation, since T_h is equivalent to the cluster mean temperature) one concludes that the characteristic radius r_c, and therefore the temperature profile, does not simply scale with the virial radius of the cluster.

3. ENTROPY PROFILES

The ICM entropy distribution has been shown to be a very powerful tool to study non-gravitational processes such as radiative cooling, preheating and feedback from supernovae and active galactic nuclei (e.g., Voit (2004)).
For our sample of CF clusters we have derived entropy profiles and studied they scaling properties (Piffaretti et al. (2005)). We define the entropy as $S = kT/n_{\rm e}^{2/3}$, where T and $n_{\rm e}$ are the deprojected electron temperature and density, respectively. In the standard self-similar scenario, one predicts $S \propto h^{-4/3}(z)\,T$, where $h^2(z) = \Omega_{\rm m}(1+z)^3 + \Omega_\Lambda$. On the other hand, recent results by Ponman et al. (2003) suggest that entropy scales with temperature as $S \propto T^{0.65}$, the so-called "entropy ramp", instead of $S \propto T$. While both scalings $S \propto h^{-4/3}(z)\,T$ and $S \propto h^{-4/3}(z)\,T^{0.65}$ considerably reduce the dispersion of the profiles, we investigated which of these scalings reduces it the most. Using $r_{\rm vir}$ to scale radii, we quantify the dispersion of the scaled profiles using the standard deviation and the mean of the scaled entropy values at a fixed scaled radius. As mean cluster temperature T, we use the mean emission-weighted temperature. The scaled entropy values are evaluated at fractions of $r_{\rm vir}$ for which no extrapolation is needed and we compute the ratio between their standard deviation σ and mean m to quantify the relative dispersion of the scaled profiles. We find that the dispersion is less if the "entropy ramp" scaling is used: $\sigma/m = 0.37$ and $\sigma/m = 0.29$ at $0.1 r_{\rm vir}$ for the $S \propto T$ and $S \propto T^{0.65}$ temperature scaling, respectively. This result does not depend on the fraction of the virial radius at which the entropy is determined and the adopted cosmology. In Fig. 2 we show entropy profiles scaled according to the "entropy ramp" relation. We fit these data with a line in log-log space (with errors in both coordinates) and find, in excellent agreement with the value found by Pratt & Arnaud (2005), a slope equal to 0.95 ± 0.02. Similarly, using *Chandra* data, Ettori et al. (2002) find a slope equal to 0.97 for the entropy profile of A 1795. Therefore, our analysis gives additional evidence for a slope close to, but slightly shallower than 1.1, the value predicted by shock dominated spherical collapse models (Tozzi & Norman (2001)). The normalization of the S-T relation we derive from the scaling of the entropy profiles is in excellent agreement with the one found by Ponman et al. (2003). Pratt et al. (2005) (see G. Pratt's proceedings of this conference), using a complementary sample of 10 nearby relaxed clusters, presented results on entropy profiles and their scaling properties in excellent agreement with ours.

4. HEATING COOLING CORES

The lack of evidence for cool gas below approximatively one third of the cluster mean temperature has motivated the development of many CF heating models. AGN heating is the most appealing candidate. In fact, most of CF clusters host an AGN with strong radio activity at their

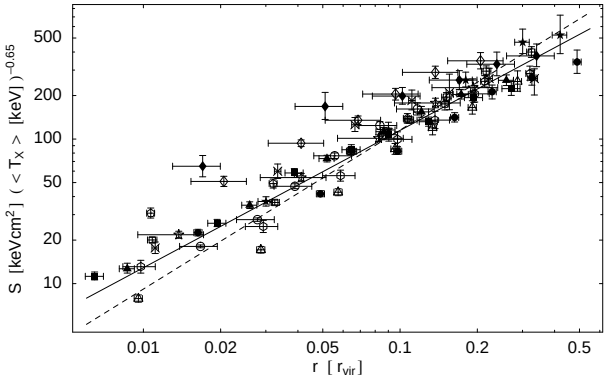

Figure 2. Entropy profiles in a SCDM50 cosmology ($\Omega_{\rm m} = 1$ with $H_0 = 50$ km s^{-1} Mpc^{-1}). The radius is scaled with the radius $r_{\rm vir}$, while the scaling $S \propto h^{-4/3}(z)\,T^{0.65}$ has been applied to the entropy values. Clusters are related to symbols as in Fig. 1. The solid line indicates the best fit power-law (best fit power index 0.95) and the dashed one the best fit power-law with the power index value fixed to 1.1, i.e. the value predicted by shock dominated spherical collapse models.

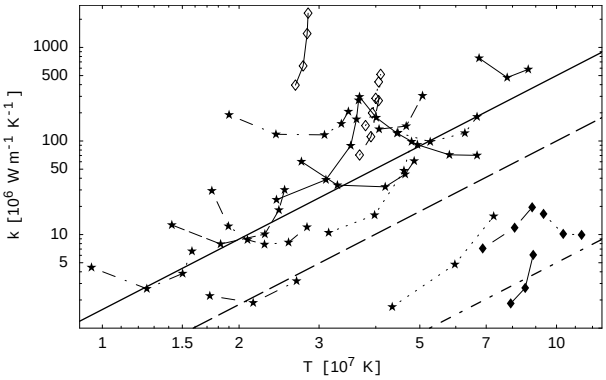

Figure 3. The conduction coefficients κ required for heat conduction to balance radiation losses as a function of temperature. The solid line is the Spitzer conductivity, the dashed lines are one fifth and one hundredth of the Spitzer conductivity, respectively. Filled diamonds represent the values for the three clusters without cooling flow (Coma, A 3266 and A 754), while open diamonds represent the values for the clusters with a shallow temperature profile (MKW 3s, Sérsic 159-3 and Hydra A). Filled stars represent the remaining clusters. Values for the same cluster are joined by a line and values are given only for bins with cooling times less than ∼30 Gyr.

centers and, most important, recent observations show that these radio sources are interacting with the ICM and are often displacing the hot gas leaving cavities in their wakes. The class of models in which the AGN energy input alone balances radiative losses is however thought to be unable to quench the CF (Brighenti & Mathews (2002); Zakamska & Narayan (2003)). Thermal conduction by electrons might also play a very important role in CFs. In Kaastra et al. (2004) we have computed, using the sample of 17 CF clusters mentioned above and in addition for 3 non-CF cluster (Coma, A 3266 and A 754), the conduction coefficients κ required to balance radiative losses completely. Our estimates of the conduction coefficients κ are shown in Fig. 3. The estimated conduction coefficients must be compared to theoretical calculations to see whether heat conduction from the outer regions can totally balance radiative losses. For a highly ionized plasma such as the ICM, the maximum rate is expected to be the Spitzer conductivity:

$$\kappa_S = \frac{1.84 \times 10^{-5}\,(T)^{5/2}}{\ln\Lambda}\,\mathrm{erg\,cm^{-1}\,s^{-1}\,K^{-1}}\,, \quad (2)$$

where $\ln\Lambda \sim 40$ is the Coulomb logarithm. In the presence of a homogeneous magnetic field, the conductivity is the Spitzer rate only along the field, but severely decreased in the transverse direction. The suppression of conductivity below the Spitzer rate, which can be written as $\kappa = f_c \times \kappa_S$, therefore depends on the strength and topology of the magnetic field. For tangled magnetic field at the level observed in CF clusters thermal conductivity is below the Spitzer level by a factor of order 10^2 to 10^3, depending on the assumed field tangling scale. Conductivity is less severely decreased if the magnetic field behaves chaotically over a wide range of scales: Narayan & Medvedev (2001) estimate that in this case conductivity is only a factor ∼5 below the Spitzer rate and Gruzinov (2002) pointed out that the effective heat conduction in a random variable magnetic field is boosted to a factor of 3 below the Spitzer value. In Fig. 3 we therefore show the Spitzer conductivity $\kappa_{\rm S}$, $\kappa_{\rm S}/5$ and $\kappa_{\rm S}/100$ for comparison. For the three non cooling clusters we find very low values for the conductivity coefficients: the absence of significant cooling allows even inefficient heat conduction to remove temperature inhomogeneities. For the cooling clusters we see that clusters with shallow temperature profile show a very different trend and relatively high conductivity because of the small temperature gradients. Since the thermal conductivity in the ICM is estimated to be below the Spitzer rate by at least a factor of 3-5, we conclude that in general heat conduction alone is insufficient to balance radiative losses in cooling clusters. The exception is the CF cluster A 399 (see the 3 data points in the lower right corner of Fig. 3), where conduction is very efficient, owing to its relatively high temperature and very steep temperature profile. In addition to this observational evidence, it has been shown that models with heat conduction as the only heating source are unstable (Soker (2003)).

While models with either heat conduction or AGN feedback acting as the sole heating source fail in supplying the needed heat to balance radiative cooling losses, models with both these mechanisms acting together are more attractive due to the complementary nature of the two processes: thermal conduction is effective/ineffective in the outer/inner regions of the cluster and AGN heating effective/ineffective in the inner/outer part. Ruszkowski & Begelman (2002) (RB02) have recently proposed such a model. The ICM density and temperature evolved according to their model reach a final stable configuration in agreement with the general shape of observed density and temperature profiles in CF clusters. RB02's model is the

only proposed theoretical model that can be effectively tested against observations. Unfortunately this has only been done for the cluster M87 (Ghizzardi et al. (2004)) and it is not clear whether the model can give a satisfactory explanation to the dynamics of CF clusters in general. In Piffaretti & Kaastra (2005) we have addressed the latter question using our sample of CF clusters observed with *XMM-Newton* (see Table 1 for the objects we used for this analysis). The heating sources present in the effervescent heating model are: AGN feedback, thermal conduction and the energy due to the inflow of the gas. In Piffaretti & Kaastra (2005) we have taken into account all of then, but here we present results for models without gas mass dropout of outflow. In this case, of the thermodynamic equations describing the ICM, only the energy equation is of interest. Assuming spherical symmetry, we have:

$$H = \varepsilon - \varepsilon_{cond}. \tag{3}$$

$\varepsilon = n_{\rm e}^2 \Lambda(T)$ ($n_{\rm e}$ is the electron density and $\Lambda(T)$ the cooling function) is the plasma emissivity and ε_{cond} is the heating due to thermal conduction, which is given by:

$$\varepsilon_{cond} = \frac{1}{r^2}\frac{d}{dr}\left(r^2 \kappa \frac{dT}{dr}\right), \tag{4}$$

where $\kappa = f_c \times \kappa_S$ is the conductivity and T is the gas temperature. As a consequence, H in the energy equation (Eq. 3) is an extra heating term, which, in the effervescent heating model developed in RB02, is provided by buoyant bubbles injected into the ICM by the central AGN.
The suppression of thermal conduction is taken into account by investigating models with thermal conduction varying from zero to the maximum level of $1/3$ times the Spitzer value ($0 \leq f_c \leq 1/3$). The RB02 heating function H^{AGN} can be expressed according to:

$$H^{AGN} = -h(r)\left(\frac{p}{p_0}\right)^{(\gamma_b - 1)/\gamma_b} \frac{1}{r}\frac{d\ln p}{d\ln r}, \tag{5}$$

with

$$h(r) = \frac{L}{4\pi r^2}\left(1 - e^{-r/r_0}\right) q^{-1} \tag{6}$$

and where

$$q = \int_0^{+\infty} \left(\frac{p}{p_0}\right)^{(\gamma_b - 1)/\gamma_b} \frac{1}{r}\frac{d\ln p}{d\ln r}\left(1 - e^{-r/r_0}\right) dr\,. \tag{7}$$

p_0 is some reference ICM pressure (here its value at the cluster center) and L the *time-averaged* luminosity of the central source. The term $1 - \exp(-r/r_0)$ introduces an inner cutoff which fixes the scale radius where the bubbles start rising in the ICM.
From the observed gas temperature and density profiles the required extra heating H can be computed for fixed values of the conduction efficiency f_c and then fitted using the AGN heating function H^{AGN}. For each bin with measured gas density and temperature we compute the gas emissivity ε. The conductive heat ε_{cond} is computed using the temperature profile given in Eq. 1 and then evaluated at the radius where the gas emissivity is computed, to finally obtain, through Eq. 3, the extra heating H.
Finally the AGN heating function given in Eq. 5 is fitted to the extra heating data points using a χ^2 minimization. The gas pressure and pressure gradients in Eq. 5 are evaluated using Eq. 1 and a β-model for the gas density profile. For any fixed f_c parameters are therefore r_0 and the luminosity of the central AGN L. The bubbles adiabatic index γ_b is fixed to $4/3$.
In Fig. 4 we illustrate results for the cluster A 1795 and discuss them in the following, since the model outcome for this object highlights the features also found for most of the clusters in the sample. $f_{\rm c} = 1/3$ is the maximum value we consider and therefore corresponds to the maximum energy yield by heat conduction from the outer parts of the cluster. From a visual inspection of Fig. 4 it is clear that heat conduction is not able to lower the extra heating in the outermost bins. As a consequence, if the extra heating curve is fitted with Eq. 5 the resulting best fit parameter r_0 (the scale radius where the bubbles start rising in the ICM) is unphysically large ($r_0 = 176$ kpc) and the *time-averaged* AGN luminosity $L = 3.3 \times 10^{45}\,{\rm erg\,s^{-1}}$ quite large. On the other hand, if the effervescent heating is assumed to be efficient in the region within the cooling radius only, one can notice that heat conduction is effective in lowering the extra heating so that the resulting extra heating curve is monotonically falling with radius. In this case one therefore expects that the extra heating supplied by the raising relativistic bubbles must be distributed over smaller distances and that the total AGN energy output is lower. This is indeed reflected in the much different best fit parameters $r_0 = 14$ kpc and $L = 8 \times 10^{44}\,{\rm erg\,s^{-1}}$. This feature indicates that, as expected, the effervescent heating model strongly depends on how much and at which radial distance heat conduction is efficient. Therefore, we have performed fits using the whole observed radial range and the radial range delimited by the cooling radius.
Another common feature is the effect of the variation of the conduction efficiency. If $f_{\rm c} = 0$ the extra heating curve is simply equal to the gas emissivity and the increase of $f_{\rm c}$ from 0 to $1/3$ gives a decrease of the extra heating curve from the emissivity curve to the data points marked in Fig. 4. The increase of $f_{\rm c}$ should hence lead to a decrease of the AGN energy requirement. In fact we find that, within the cooling radius, both *time-averaged* AGN luminosity and inner cutoff radius r_0 decrease monotonically with increasing $f_{\rm c}$. This opposite effect is seen if the fits are performed over the whole radial range: an increase of $f_{\rm c}$ leads to an increase in both L and r_0, showing again the inadequacy of applying the model over the whole radial range.
For the majority of the objects in our sample we find that the effervescent heating model provides results when the radial range used to fit the extra heating curve with Eq. 5 is not simply the whole range observed but the radial range inside the cooling region. For A 399 no results are obtained for neither of the two radial ranges. The reason for the lack of convergence of the fits is that in A 399 heat conduction is very efficient, owing to its relatively high temperature and very steep temperature profile. The results for the sample are summarized in Table 1. While for most of the clusters we find a solution for L and r_0

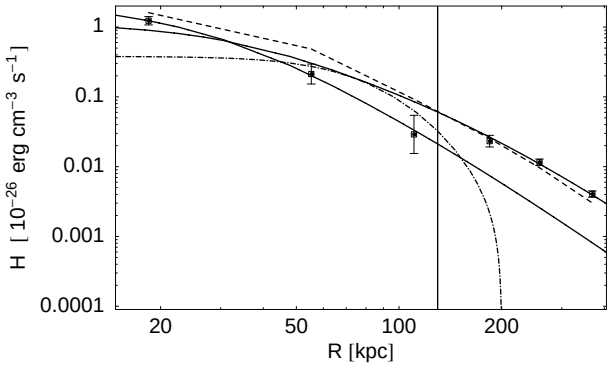

Figure 4. Energy requirements in A 1795: the plasma emissivity (for simplicity shown by the dashed line joining the data points) and heating due to thermal conduction (dot-dashed line) as a function of radius. The he extra heating curve (open squares) is determined by $f_{\rm c}\times$ Spitzer. Here $f_{\rm c} = 1/3$, the maximum value allowed in the models. The three bins inside the cooling radius (vertical line) alone are best fitted by an inner cutoff radius $r_0 = 14$ kpc and time-averaged AGN luminosity $L = 8.0 \times 10^{44}\,{\rm erg\,s^{-1}}$. For the same model all six bins are best fitted by an unphysical $r_0 = 179$ kpc and very high AGN luminosity $L = 3.3 \times 10^{45}\,{\rm erg\,s^{-1}}$. The two solid curves are the best fit functions for the two cases.

Table 1. The results for the effervescent heating model with no mass dropout (see text for comment).

Cluster	$f_{\rm c}^{\rm min,max}$	$r_0^{\rm min,max}$ (kpc)	$L^{\rm min,max}$ (erg s^{-1})
NGC 533*	0.00,0.26	0.3,1.5	$1.6, 2.6 \times 10^{42}$
Virgo*	0.03,0.26	0.6,18	$3.8, 21 \times 10^{42}$
A 262*	0.12,0.33	6.6,60	$8.1, 47 \times 10^{42}$
Sérsic 159*	0.00,0.33	22,23	$5.8, 5.8 \times 10^{44}$
MKW 9*	0.08,0.10	15,15	$5.7, 6.5 \times 10^{42}$
2A 0335*	0.00,0.33	15,16	$6.1, 6.8 \times 10^{44}$
MKW 3s	0.00,0.33	37,94	$4.3, 5.8 \times 10^{44}$
A 2052	0.00,0.33	6.6,21	$2.6, 3.4 \times 10^{44}$
A 4059*	0.00,0.33	4.7,54	$7.4, 50 \times 10^{43}$
Hydra A*	0.00,0.33	27,29	$7.0, 7.7 \times 10^{44}$
A 496*	0.07,0.28	11,86	$1.2, 5.7 \times 10^{44}$
A 3112	0.00,0.33	30,59	$1.3, 1.4 \times 10^{45}$
A 1795*	0.00,0.33	14,49	$8.0, 24 \times 10^{44}$
A 399	-	-	-
Perseus*	0.01,0.18	40,73	$1.6, 2.5 \times 10^{45}$
A 1835*	0.00,0.33	33.2,38	$1.0, 1.1 \times 10^{46}$

for every value of $0 < f_c < 1/3$, for some objects the fits converge only for models with f_c in a narrower interval ($f_{\rm c}^{\rm min}$-$f_{\rm c}^{\rm max}$, see Table 1). In particular in clusters where conduction is high (MKW 9 and Perseus), the solutions have conduction efficiency substantially lower than the maximum allowed value $f_c = 1/3$. In Sérsic 159−3, 2A 0335+096, Hydra A, A 3112 and A 1835 the conductivity yield is low and, as expected, different models (i.e. different values of f_c) give almost identical results.

It is crucial to highlight the trend of the best fit parameters of the different models with model parameter f_c. For most of the clusters the model with $f_{\rm c} = f_{\rm c}^{\rm max}$ is the one for which the values for both L and r_0 are smallest and for $f_{\rm c} = f_{\rm c}^{\rm min}$ the largest ($L^{\rm min,max}$ and $r_0^{\rm min,max}$ in Table 1). In addition L and r_0 vary monotonically with f_c within these limits. The clusters which exhibit this trend are labeled by an asterisk Table 1. For MKW 3s, A 2052 and A 3112 the trend just described is reversed. In these objects heat conduction lowers the extra heating curve especially in the cluster center. This implies more and more flattening of the extra heating curve at the center with increasing f_c which is finally reflected in the increase of both r_0 and L. Our conclusions are:

- for 4 clusters (Sérsic 159−3, 2A 0335+096, Hydra A and A 1835) the conductivity yield is extremely low and, as expected, different models (i.e. different values of f_c) give almost identical results,
- for 3 objects (MKW 3s, A 2052 and A 3112) we find that heat conduction plays an important role only at the cluster center and that, as a consequence, the trend between the fitted AGN parameters and conduction efficiency is not the one expected (i.e. conduction and AGN feedback do not co-operate),
- for one object (A 399) we do not find any solution for the effervescent heating model because heat conduction is very efficient,
- for the remaining 8 clusters (NGC 533, Virgo, A 262, MKW 9, A 4059, A 496, A 1795 and Perseus) conduction and AGN feedback are found to be co-operating as expected.

Since it has been shown that AGN heating alone is not able to quench CFs, it is fair to assume that thermal conduction, although operating at different rates from cluster to cluster, must play an important role as a heating mechanism, at least, of course, in the framework of the effervescent heating model. While this is found for 8 clusters in our sample, we have shown that heat conduction is either completely unrelevant in 4 clusters, too high for one object or high enough to play an important role but peaked at the cluster center in 3 clusters. Hence, if we assume that the effervescent heating provides a satisfactory explanation for the observed structure of CF clusters only in the case when AGN and conduction heating are effectively co-operating, we conclude that for half of the objects in the sample the effervescent heating does not provide a satisfactory explanation.

These findings prompt us to posit that, at least for

these objects, the description of their thermal structure through a *steady state* solution of the thermodynamic equations is not viable and that we are observing them at an evolutionary stage far from equilibrium. A clearer picture can be of course achieved by studying a much larger sample using the procedure employed in this work.

ACKNOWLEDGMENTS

This work is based on observations obtained with *XMM-Newton*, an ESA science mission with instruments and contributions directly funded by ESA Member States and the USA (NASA). RP acknowledges support from the Swiss National Science Foundation and the Tiroler Wissenschaftsfond. SRON is supported financially by NWO, the Netherlands Foundation for Scientific Research.

REFERENCES

Blanton, E. L. 2004, The Riddle of Cooling Flows in Galaxies and Clusters of galaxies

Brighenti, F., & Mathews, W. G. 2002, ApJ, 573, 542

De Grandi, S., & Molendi, S. 2002, ApJ, 567, 163

Ettori, S., Fabian, A. C., Allen, S. W., & Johnstone, R. M. 2002a, MNRAS, 331, 635

Ghizzardi, S., Molendi, S., Pizzolato, F., & De Grandi, S. 2004, ApJ, 609, 638

Gruzinov, A. 2002, astro-ph/0203031

Kaastra, J. S., Tamura, T., Peterson, J. R., et al. 2004, A&A, 413, 415

Markevitch, M., Forman, W. R., Sarazin, C. L., & Vikhlinin, A. 1998, ApJ, 503, 77

Narayan, R., & Medvedev, M. V. 2001, ApJ, 562, L129

Peterson, J. R., Kahn, S. M., Paerels, F. B. S., et al. 2003, ApJ, 590, 207

Piffaretti, R., Jetzer, Ph., Kaastra, J. S., & Tamura, T. 2005, A&A, 433, 101

Piffaretti, R. & Kaastra, J. S. 2005, submitted to A&A

Ponman, T. J., Sanderson, A. J. R., & Finoguenov, A. 2003, MNRAS, 343, 331

Pratt, G. W., & Arnaud, M. 2005, A&A, 429, 791

Pratt, G. W., Arnaud, M., & Pointecouteau, E. 2005, to appear in A&A, astro-ph/0508234

Ruszkowski, M., & Begelman, M. C. 2002, ApJ, 581, 223 (RB02)

Soker, N. 2003, MNRAS, 342, 463

Tozzi, P., & Norman, C. 2001, ApJ, 546, 63

Vikhlinin, A., Markevitch, M., Murray, S. S., Jones, C., Forman, W., & Van Speybroeck, L. 2005, ApJ, 628, 655

Voit, M. G. 2005, Rev. Mod. Phys., 77, 207

Zakamska, N. L., & Narayan, R. 2003, ApJ, 582, 162